

# Local discontinuous Galerkin method for the numerical solution of fractional compartmental model with application in pharmacokinetics

Hadi Mohammadi-Firouzjaei<sup>†</sup>, Mona Adibi<sup>‡</sup>, Hojatollah Adibi<sup>§\*</sup>

<sup>†,§</sup>*Department of Applied Mathematics, Faculty of Mathematics and Computer Sciences, Amirkabir University of Technology, No. 424, Hafez Ave., 15914, Tehran, Iran*

<sup>‡</sup>*Department of Health, Safety and Environment (Department of Health)*

*Amirkabir University of Technology, No. 424, Hafez Ave., 15914, Tehran, Iran*

*Email(s): hmohamadi.math@aut.ac.ir; adibipharmd@gmail.com, adibih@aut.ac.ir*

---

**Abstract.** This paper provides a numerical solution for the fractional multi-compartmental models which are applied in pharmacokinetics. We implement the local discontinuous Galerkin method for these fractional models with the upwind numerical fluxes. To obtain high-order results with adequate accuracy, the third-order approximation polynomials are used. Finally, to validate the scheme, the results are compared with the solutions of a semi-analytical method.

*Keywords:* Local discontinuous Galerkin method, Fractional compartmental model, Pharmacokinetics.

*AMS Subject Classification 2010:* 34A08, 92C45, 65L60, 26A33.

---

## 1 Introduction

Pharmacokinetics is the study of the fate of foreign chemicals also known as xenobiotics in the body. During the transit through and out of the living organism, xenobiotics go through four different phases of kinetics identified as Absorption, Distribution, Biotransformation/Metabolism and Excretion (ADME). Mathematical equations and simulating models are implemented in pharmacokinetics in order to explain the time course for each phase of ADME of xenobiotics throughout the body. The data achieved helps us determine the onset of action, duration of effects, and intensity of therapeutic and toxic properties of xenobiotics [19].

The Michaelis-Menten kinetics was one of the first equations for explaining enzyme kinetics [13]. Nowadays, numerous mathematical methods are utilized in pharmacokinetics to predict how the living organism handles xenobiotics; in addition, on the basis of mathematical modelling or physiological

---

\*Corresponding author.

Received: 10 September 2021/ Revised: 25 September 2021/ Accepted: 29 September 2021

DOI: 10.22124/jmm.2021.20561.1790

properties the organism is regarded as one or more homogeneous compartments. In a single-compartment model, the body acts as a uniform compartment where the uptake, distribution, and elimination of xenobiotics from the central compartment to the peripheral compartments is instantaneous, uniform and homogeneous following first-order kinetics such as administering a bolus intravenous injection. The central compartment mirrors the plasma and well-perfused tissues such as the heart and liver, while the peripheral compartments reflect less perfused tissues. Contrarily, for many xenobiotics the diffusion to the peripheral compartments is non-homogeneous and slow, therefore further compartments should be taken into account [16]. In a two-compartment model, the xenobiotic is distributed in the plasma rapidly and homogeneously while gradually diffusing into and out from the tissues [20]. Therefore unlike the single compartment model, xenobiotics exhibiting two-compartment model pharmacokinetics do not achieve a rapid equilibrium throughout the body [20].

Einstein's explanation of Brownian motion provided one of the cornerstones for drug diffusion between compartments. This random and rapid motion of drug mass from high to low concentrations is described by the diffusion equation and serves as a mathematical model for random processes where the Mean Squared Displacement (MSD) is linear over time [7]. However, several biological systems exhibit a non-linear diffusion process, known as an anomalous diffusion or non-Fickian diffusion process, such as the ion channels in the plasma membrane [23]. A study conducted by Amanda Diez Fernandez et al., for the purpose of safe and effective drug target therapy of Doxorubicin encapsulated in mesoporous silica nanospheres showed that the diffusion of Doxorubicin drug molecules in a nano-film of water confined between two planar silica surfaces is non-Brownian, non-Gaussian. In this study, by using computer simulation and single molecule tracking methods it was observed that prolonged periods of adsorption of Doxorubicin drug molecules on silica surfaces, leads to ageing which is seen when the diffusion of drug molecules is intermittently restrained for a lengthy amount of time of theoretically infinite duration, causing the anomalous diffusion of Doxorubicin drug molecules [8].

In recent years, the use of fractional operators in models describing the dynamics of biological phenomena has received much attention. Dokoumetzidis and Macheras [5] used the concepts of the fractional calculus and introduced pharmacokinetic models for drug dissolution/release and drug disposition. Moreover, there are some researches focused on parameter estimation of the models [6, 18] which also numerically solve these types of models.

Another way to discretize the fractional temporal term is to use the discontinuous Galerkin (DG) method. To solve differential equations with higher derivatives, other type of DG methods like Local discontinuous Galerkin (LDG) was introduced [3]. The LDG method as one of the extensions of the DG method has been extensively studied for solving fractional ODEs and PDEs [4, 9, 15]. Likewise, DG method, this method provides some advantages such as good stability, easily designing for any order of accuracy and achieving the locally order of accuracy in each element, excellent parallel efficiency and locally conservative which drawn a lot of interests in many fields. Deng and Hesthaven [4] developed a LDG scheme for fractional ODEs. Mustapha and McLean utilized DG for a fractional diffusion equations [15]. The main purpose of this work is to use LDG scheme for some fractional multi-compartment models and in order to validate the scheme, we compare the results obtained by the LDG scheme with a semi-analytic approach based on the numerical inverse Laplace transform (NILT) method. This semi-analytic approach is widely used for fractional ODEs [6, 18, 22], PDEs [12, 14] and integro-differential equations [11].

We start with the two-compartment model. Denote the mass or molar amounts of drug in  $j$ -th com-

partment by  $\rho_j, j = 1, 2$ . The general form of the two-compartment model [6, 18] is introduced as follows

$$\begin{aligned} \frac{d\rho_1(t)}{dt} &= -k_{10} {}^C D_t^{1-\alpha_{10}} \rho_1(t) - k_{12} {}^C D_t^{1-\alpha_{12}} \rho_1(t) + k_{21} {}^C D_t^{1-\alpha_{21}} \rho_2(t) + u_1(t), \\ \frac{d\rho_2(t)}{dt} &= -k_{20} {}^C D_t^{1-\alpha_{20}} \rho_2(t) - k_{21} {}^C D_t^{1-\alpha_{21}} \rho_2(t) + k_{12} {}^C D_t^{1-\alpha_{12}} \rho_1(t) + u_2(t), \end{aligned} \tag{1}$$

in which the constants  $k_{xy}$ , control the mass transfer between compartments  $x$  and  $y$  corresponds to the transfer from compartment  $x$  (the source) to compartment  $y$  (the target) and  $k_{x0}$  corresponds to the elimination from compartment  $x$ . The infusion rate in compartment  $j$ , is denoted by  $u_j(t)$ .

In most cases, the following model [6, 18] is considered

$$\begin{aligned} \frac{d\rho_1(t)}{dt} &= -(k_{10} + k_{12}) \rho_1(t) + k_{21} {}^C D_t^{1-\alpha} \rho_2(t) + u_1(t), \\ \frac{d\rho_2(t)}{dt} &= k_{12} \rho_1(t) - k_{21} {}^C D_t^{1-\alpha} \rho_2(t). \end{aligned} \tag{2}$$

The rest of the paper is arranged as follows: Section 2, gives some definitions and notations. Section 3 provides to introduce the LDG method for the general systems (1) and (2). In Section 4, we give some numerical experiments and compare the results of the proposed scheme with a semi-analytic method based on the Laplace transform (LT), called the Talbot method.

## 2 Preliminaries

This section, provides useful definitions and notations. We start with the standard calculus and follow the section by some required materials in fractional calculus.

The  $m$ -th repeated integral of a function  $f(t)$ , the Cauchy formula, is

$${}_{t_0} D_t^{-m} f(t) = \int_{t_0}^t \int_{t_0}^{\zeta_1} \dots \int_{t_0}^{\zeta_{m-1}} f(\zeta_m) d\zeta_m \dots d\zeta_2 d\zeta_1 = \frac{1}{(m-1)!} \int_{t_0}^t (t-\zeta)^{m-1} f(\zeta) d\zeta, \quad m \in \mathbb{Z}^+, \quad t_0 < t.$$

Also, the  $m$ -th derivative of a function  $f(t)$  is denoted by  $\frac{d^m}{dt^m} f(t)$ .

On the other hand, the fractional (left Riemann-Liouville (RL)) integral of order  $\alpha \in \mathbb{R}^+$  is defined as

$${}_{t_0} D_t^{-\alpha} f(t) = \frac{1}{\Gamma(\alpha)} \int_{t_0}^t (t-\zeta)^{\alpha-1} f(\zeta) d\zeta, \quad t_0 < t.$$

The left fractional Riemann-Liouville (RL) derivative of order  $(m - \alpha)$  is

$${}_{t_0} D_t^{m-\alpha} f(t) = \frac{1}{\Gamma(\alpha)} \frac{d^m}{dt^m} \int_{t_0}^t (t-\zeta)^{\alpha-1} f(\zeta) d\zeta, \quad 0 < \alpha < 1,$$

and when  $m = 1$

$${}_{t_0} D_t^{1-\alpha} f(t) = \frac{1}{\Gamma(\alpha)} \frac{d}{dt} \int_{t_0}^t (t-\zeta)^{\alpha-1} f(\zeta) d\zeta, \quad 0 < \alpha < 1.$$

One can see that  ${}_t D_t^{1-\alpha} f(t) = \frac{d}{dt} {}_t D_t^{-\alpha} f(t)$ . Note that, the RL derivative of a constant value is not zero and due to this property scientists and engineers often use another fractional temporal derivative known as the Caputo definition

$${}_t^C D_t^{m-\alpha} f(t) = \frac{1}{\Gamma(\alpha)} \int_{t_0}^t (t-\zeta)^{\alpha-1} \frac{d^m}{d\zeta^m} f(\zeta) d\zeta, \quad 0 < \alpha < 1,$$

and when  $m = 1$

$${}_t^C D_t^{1-\alpha} f(t) = \frac{1}{\Gamma(\alpha)} \int_{t_0}^t (t-\zeta)^{\alpha-1} \frac{d}{d\zeta} f(\zeta) d\zeta, \quad 0 < \alpha < 1.$$

It can be seen that  ${}_t^C D_t^{1-\alpha} f(t) = {}_t D_t^{-\alpha} \frac{d}{dt} f(t)$  which is required in the implementation of the LDG scheme. We also need to define the Mittag-Leffler functions for their importance in fractional calculus.

**Definition 1.** The one-parameter Mittag-Leffler function, is defined as [17]:

$$E_{\alpha}(t) = \sum_{k=0}^{\infty} \frac{t^k}{\Gamma(\alpha k + 1)}, \quad \alpha > 0, \quad \alpha \in \mathbb{R}, \quad t \in \mathbb{C}. \quad (3)$$

**Definition 2.** The generalized Mittag-Leffler function, as a two-parameter function is defined by [17]:

$$E_{\alpha, \beta}(t) = \sum_{k=0}^{\infty} \frac{t^k}{\Gamma(\alpha k + \beta)}, \quad \alpha, \beta > 0, \quad \alpha, \beta \in \mathbb{R}, \quad t \in \mathbb{C}. \quad (4)$$

### 3 Local discontinuous Galerkin schemes

The goal of this part is to present the LDG scheme for solving Eqs. (1) and (2). We follow a similar procedure presented in [4] and use some definitions and notations therein.

**Case 1 | Eq. (1) :** In order to implement the LDG scheme, the system of Eqs. (1) is rewritten as

$$\begin{cases} q_1(t) = -k_{10} {}_0 D_t^{-\alpha_{10}} q_1(t) - k_{12} {}_0 D_t^{-\alpha_{12}} q_1(t) + k_{21} {}_0 D_t^{-\alpha_{21}} q_2(t) + u_1(t), \\ q_1(t) - \frac{d\rho_1(t)}{dt} = 0, \\ q_2(t) = -k_{20} {}_0 D_t^{-\alpha_{20}} q_2(t) - k_{21} {}_0 D_t^{-\alpha_{21}} q_2(t) + k_{12} {}_0 D_t^{-\alpha_{12}} q_1(t) + u_2(t), \\ q_2(t) - \frac{d\rho_2(t)}{dt} = 0. \end{cases} \quad (5)$$

Lets define  $\Omega_t = [0, T]$  and  $0 = t_{\frac{1}{2}} < t_{\frac{3}{2}} < \dots < t_{n-1} < t_{n+\frac{1}{2}} = T$ . The mesh can be defined as  $S = \left\{ I_i = (t_{i-\frac{1}{2}}, t_{i+\frac{1}{2}}), \quad i = 1, \dots, n \right\}$  and  $\tau_i = t_{i+\frac{1}{2}} - t_{i-\frac{1}{2}}$  and also  $\tau = \max_{0 \leq i \leq n} \tau_i$ .

Integrating equations (5) over an arbitrarily interval  $I_i$  with respect to weight functions  $\eta_j(t)$ ,  $j =$

1, 2, 3, 4 and applying integration by parts yield the following weak formulation

$$\left\{ \begin{array}{l} (q_1(t), \eta_1(t))_{I_i} = -k_{10} ({}_0D_t^{-\alpha_{10}} q_1(t), \eta_1(t))_{I_i} - k_{12} ({}_0D_t^{-\alpha_{12}} q_1(t), \eta_1(t))_{I_i} \\ \quad + k_{21} ({}_0D_t^{-\alpha_{21}} q_2(t), \eta_1(t))_{I_i} + (u_1(t), \eta_1(t))_{I_i}, \\ (q_1(t), \eta_2(t))_{I_i} + (\rho_1(t), \frac{d\eta_2(t)}{dt})_{I_i} - \rho_1(t_{i+\frac{1}{2}}) \eta_2(t_{i+\frac{1}{2}}) + \rho_1(t_{i-\frac{1}{2}}) \eta_2(t_{i-\frac{1}{2}}) = 0, \\ (q_2(t), \eta_3(t))_{I_i} = -k_{20} ({}_0D_t^{-\alpha_{20}} q_2(t), \eta_3(t))_{I_i} - k_{21} ({}_0D_t^{-\alpha_{21}} q_2(t), \eta_3(t))_{I_i} \\ \quad + k_{12} ({}_0D_t^{-\alpha_{12}} q_1(t), \eta_3(t))_{I_i} + (u_2(t), \eta_3(t))_{I_i}, \\ (q_2(t), \eta_4(t))_{I_i} + (\rho_2(t), \frac{d\eta_4(t)}{dt})_{I_i} - \rho_2(t_{i+\frac{1}{2}}) \eta_4(t_{i+\frac{1}{2}}) + \rho_2(t_{i-\frac{1}{2}}) \eta_4(t_{i-\frac{1}{2}}) = 0, \end{array} \right. \quad (6)$$

where  $(u(t), v(t))_{I_i} = \int_{t_{i-\frac{1}{2}}}^{t_{i+\frac{1}{2}}} u(t)v(t) dt$ . Now, let's define broken Sobolev spaces as

$$L^2(\Omega_t, S) := \{v : \Omega_t \rightarrow \mathbb{R} \mid v|_{I_i} \in L^2(I_i), \quad i = 1, \dots, n\}, \quad (7)$$

and

$$H^1(\Omega_t, S) := \{v : \Omega_t \rightarrow \mathbb{R} \mid v|_{I_i} \in H^1(I_i), \quad i = 1, \dots, n\}. \quad (8)$$

In the current paper, the following finite dimensional subspace is considered

$$\mathcal{D}^p = \{v : \Omega_t \rightarrow \mathbb{R} \mid v|_{I_i} \in P^p(I_i), \quad i = 1, \dots, n\} \subset H^1(\Omega_t, S), \quad (9)$$

where  $P^p(I_i)$  is the polynomial of degree less than or equal to  $p$  on  $I_i$ .

Denote  $(\rho_{\tau,1}, \rho_{\tau,2}, q_{\tau,1}, q_{\tau,2}) \in V$  the approximation of  $(\rho_1, \rho_2, q_1, q_2)$ , in functional space  $V = \mathcal{D}^p \times \mathcal{D}^p \times \mathcal{D}^p \times \mathcal{D}^p$  and  $(\eta_{\tau,1}, \eta_{\tau,2}, \eta_{\tau,3}, \eta_{\tau,4})$  the approximation of  $(\eta_1, \eta_2, \eta_3, \eta_4)$ , in the same functional space. Substituting  $(\rho_{\tau,1}, \rho_{\tau,2}, q_{\tau,1}, q_{\tau,2})$  and  $(\eta_{\tau,1}, \eta_{\tau,2}, \eta_{\tau,3}, \eta_{\tau,4})$  for  $(\rho_1, \rho_2, q_1, q_2)$  and  $(\eta_1, \eta_2, \eta_3, \eta_4)$ , respectively, yields the following discontinuous Galerkin formulation as

$$\left\{ \begin{array}{l} (q_{\tau,1}(t), \eta_{\tau,1}(t))_{I_i} = -k_{10} ({}_0D_t^{-\alpha_{10}} q_{\tau,1}(t), \eta_{\tau,1}(t))_{I_i} - k_{12} ({}_0D_t^{-\alpha_{12}} q_{\tau,1}(t), \eta_{\tau,1}(t))_{I_i} \\ \quad + k_{21} ({}_0D_t^{-\alpha_{21}} q_{\tau,2}(t), \eta_{\tau,1}(t))_{I_i} + (u_{\tau,1}(t), \eta_{\tau,1}(t))_{I_i}, \\ (q_{\tau,1}(t), \eta_{\tau,2}(t))_{I_i} + (\rho_{\tau,1}(t), \frac{d\eta_{\tau,2}(t)}{dt})_{I_i} - \rho_{\tau,1}(t_{i+\frac{1}{2}}) \eta_{\tau,2}(t_{i+\frac{1}{2}}) + \rho_{\tau,1}(t_{i-\frac{1}{2}}) \eta_{\tau,2}(t_{i-\frac{1}{2}}) = 0, \\ (q_{\tau,2}(t), \eta_{\tau,3}(t))_{I_i} = -k_{20} ({}_0D_t^{-\alpha_{20}} q_{\tau,2}(t), \eta_{\tau,3}(t))_{I_i} - k_{21} ({}_0D_t^{-\alpha_{21}} q_{\tau,2}(t), \eta_{\tau,3}(t))_{I_i} \\ \quad + k_{12} ({}_0D_t^{-\alpha_{12}} q_{\tau,1}(t), \eta_{\tau,3}(t))_{I_i} + (u_{\tau,2}(t), \eta_{\tau,3}(t))_{I_i}, \\ (q_{\tau,2}(t), \eta_{\tau,4}(t))_{I_i} + (\rho_{\tau,2}(t), \frac{d\eta_{\tau,4}(t)}{dt})_{I_i} - \rho_{\tau,2}(t_{i+\frac{1}{2}}) \eta_{\tau,4}(t_{i+\frac{1}{2}}) + \rho_{\tau,2}(t_{i-\frac{1}{2}}) \eta_{\tau,4}(t_{i-\frac{1}{2}}) = 0. \end{array} \right. \quad (10)$$

Note that implementing the DG method, allows a function  $v_h$  to be discontinuous across the face (boundary of each element). If so, two different values exist at the interface between two elements as:

$$v_h^-(t_{i+\frac{1}{2}}) = \lim_{t \nearrow t_{i+\frac{1}{2}}} v_h(t), \quad v_h^+(t_{i+\frac{1}{2}}) = \lim_{t \searrow t_{i+\frac{1}{2}}} v_h(t). \quad (11)$$

In the current paper, we use some numerical fluxes, presented by Cockburn et al. [1, 2] and replace the values of  $\rho_{\tau,1}$  and  $\rho_{\tau,2}$  by the following fluxes

$$\rho_{\tau,j}(t_{i\pm\frac{1}{2}}) = h_j(\rho_{\tau,j}^-(t_{i\pm\frac{1}{2}}), \rho_{\tau,j}^+(t_{i\pm\frac{1}{2}})) = \rho_{\tau,j}^-(t_{i\pm\frac{1}{2}}), \quad j = 1, 2. \quad (12)$$

Utilizing these numerical fluxes, the LDG formulation results in

$$\left\{ \begin{array}{l} (q_{\tau,1}(t), \eta_{\tau,1}(t))_{I_i} = -k_{10} ({}_0D_t^{-\alpha_{10}} q_{\tau,1}(t), \eta_{\tau,1}(t))_{I_i} - k_{12} ({}_0D_t^{-\alpha_{12}} q_{\tau,1}(t), \eta_{\tau,1}(t))_{I_i} \\ \quad + k_{21} ({}_0D_t^{-\alpha_{21}} q_{\tau,2}(t), \eta_{\tau,1}(t))_{I_i} + (u_{\tau,1}(t), \eta_{\tau,1}(t))_{I_i}, \\ (q_{\tau,1}(t), \eta_{\tau,2}(t))_{I_i} + (\rho_{\tau,1}(t), \frac{d\eta_{\tau,2}(t)}{dt})_{I_i} - \rho_{\tau,1}^-(t_{i+\frac{1}{2}}) \eta_{\tau,2}^-(t_{i+\frac{1}{2}}) + \rho_{\tau,1}^-(t_{i-\frac{1}{2}}) \eta_{\tau,2}^+(t_{i-\frac{1}{2}}) = 0, \\ (q_{\tau,2}(t), \eta_{\tau,3}(t))_{I_i} = -k_{20} ({}_0D_t^{-\alpha_{20}} q_{\tau,2}(t), \eta_{\tau,3}(t))_{I_i} - k_{21} ({}_0D_t^{-\alpha_{21}} q_{\tau,2}(t), \eta_{\tau,3}(t))_{I_i} \\ \quad + k_{12} ({}_0D_t^{-\alpha_{12}} q_{\tau,1}(t), \eta_{\tau,3}(t))_{I_i} + (u_{\tau,2}(t), \eta_{\tau,3}(t))_{I_i}, \\ (q_{\tau,2}(t), \eta_{\tau,4}(t))_{I_i} + (\rho_{\tau,2}(t), \frac{d\eta_{\tau,4}(t)}{dt})_{I_i} - \rho_{\tau,2}^-(t_{i+\frac{1}{2}}) \eta_{\tau,4}^-(t_{i+\frac{1}{4}}) + \rho_{\tau,2}^-(t_{i-\frac{1}{2}}) \eta_{\tau,4}^+(t_{i-\frac{1}{2}}) = 0. \end{array} \right. \quad (13)$$

**Case 2 | Eq. (2) :** We do exactly the same as Eqs. (1). If so, Eqs. (2) can be rewritten as

$$\left\{ \begin{array}{l} q_1(t) = -(k_{10} + k_{12}) \rho_1(t) + k_{21} {}_0D_t^{-\alpha} q_2(t) + u_1(t), \\ q_1(t) - \frac{dq_1(t)}{dt} = 0, \\ q_2(t) = k_{12} \rho_1(t) - k_{21} {}_0D_t^{-\alpha} q_2(t), \\ q_2(t) - \frac{dq_2(t)}{dt} = 0. \end{array} \right. \quad (14)$$

Integrating equations (14) over an arbitrarily interval  $I_i$  with respect to weight functions  $\eta_j(t)$ ,  $j = 1, 2, 3, 4$  and applying integration by parts yield the following weak formulation

$$\left\{ \begin{array}{l} (q_1(t), \eta_1(t))_{I_i} = -(k_{10} + k_{12}) (\rho_1(t), \eta_1(t))_{I_i} + k_{21} ({}_0D_t^{-\alpha} q_2(t), \eta_1(t))_{I_i} + (u_1(t), \eta_1(t))_{I_i}, \\ \quad (q_1(t), \eta_2(t))_{I_i} + (\rho_1(t), \frac{d\eta_2(t)}{dt})_{I_i} - \rho_1(t_{i+\frac{1}{2}}) \eta_2(t_{i+\frac{1}{2}}) + \rho_1(t_{i-\frac{1}{2}}) \eta_2(t_{i-\frac{1}{2}}) = 0, \\ (q_2(t), \eta_3(t))_{I_i} = -k_{21} ({}_0D_t^{-\alpha} q_2(t), \eta_3(t))_{I_i} + k_{12} (\rho_1(t), \eta_3(t))_{I_i}, \\ \quad (q_2(t), \eta_4(t))_{I_i} + (\rho_2(t), \frac{d\eta_4(t)}{dt})_{I_i} - \rho_2(t_{i+\frac{1}{2}}) \eta_4(t_{i+\frac{1}{4}}) + \rho_2(t_{i-\frac{1}{2}}) \eta_4(t_{i-\frac{1}{2}}) = 0. \end{array} \right. \quad (15)$$

Now, if  $(\rho_{\tau,1}, \rho_{\tau,2}, q_{\tau,1}, q_{\tau,2}) \in V$  be the approximation of  $(\rho_1, \rho_2, q_1, q_2)$ , in functional space  $V = \mathcal{D}^p \times \mathcal{D}^p \times \mathcal{D}^p \times \mathcal{D}^p$  and  $(\eta_{\tau,1}, \eta_{\tau,2}, \eta_{\tau,3}, \eta_{\tau,4})$  the approximation of  $(\eta_1, \eta_2, \eta_3, \eta_4)$ , in the same functional space and considering the numerical fluxes (12) the following discontinuous Galerkin formulation is

obtained

$$\begin{cases} (q_{\tau,1}(t), \eta_{\tau,1}(t))_{I_i} = -(k_{10} + k_{12}) (\rho_{\tau,1}(t), \eta_{\tau,1}(t))_{I_i} + k_{21} ({}_0D_t^{-\alpha} q_{\tau,2}(t), \eta_{\tau,1}(t))_{I_i} + (u_{\tau,1}(t), \eta_{\tau,1}(t))_{I_i}, \\ (q_{\tau,1}(t), \eta_{\tau,2}(t))_{I_i} + (\rho_{\tau,1}(t), \frac{d\eta_{\tau,2}(t)}{dt})_{I_i} - \rho_{\tau,1}^-(t_{i+\frac{1}{2}}) \eta_{\tau,2}^-(t_{i+\frac{1}{2}}) + \rho_{\tau,1}^-(t_{i-\frac{1}{2}}) \eta_{\tau,2}^+(t_{i-\frac{1}{2}}) = 0, \\ (q_{\tau,2}(t), \eta_{\tau,3}(t))_{I_i} = -k_{21} ({}_0D_t^{-\alpha} q_{\tau,2}(t), \eta_{\tau,3}(t))_{I_i} + k_{12} (\rho_{\tau,1}(t), \eta_{\tau,3}(t))_{I_i}, \\ (q_{\tau,2}(t), \eta_{\tau,4}(t))_{I_i} + (\rho_{\tau,2}(t), \frac{d\eta_{\tau,4}(t)}{dt})_{I_i} - \rho_{\tau,2}^-(t_{i+\frac{1}{2}}) \eta_{\tau,4}^-(t_{i+\frac{1}{2}}) + \rho_{\tau,2}^-(t_{i-\frac{1}{2}}) \eta_{\tau,4}^+(t_{i-\frac{1}{2}}) = 0. \end{cases} \tag{16}$$

### 4 Numerical results

This section, is devoted to present the results obtained by the proposed local discontinuous Galerkin scheme. Note that all computations are carried out by using a computer with the processor Intel Core™ i7 – 6600U CPU @2.60GHz × 4 with 16 GB RAM.

Here, the rate of convergence of errors is defined as

$$Rate = (\ln(2))^{-1} \ln \left( \frac{\|e_h\|_{L_2}}{\|e_{h/2}\|_{L_2}} \right),$$

where

$$\|e_h\|_{L_2} = \left( \int_S (\tilde{\rho} - \rho)^2 dt \right)^{1/2},$$

and  $\tilde{\rho}$  and  $\rho$  are numerical and exact solutions of the equation, respectively.

**Example 1.** In this example, we consider the following equation

$$\begin{aligned} \frac{d\rho_1(t)}{dt} &= -(k_{10} + k_{12}) \rho_1(t) + k_{21} {}_0^C D_t^{1-\alpha} \rho_2(t) + g_1(t), \\ \frac{d\rho_2(t)}{dt} &= k_{12} \rho_1(t) - k_{21} {}_0^C D_t^{1-\alpha} \rho_2(t) + g_2(t). \end{aligned} \tag{17}$$

where  $\rho_1(0) = d_1, \rho_2(0) = 0, k_{10} = 1, k_{12} = 1, k_{21} = 2, d_1 = 200mg, d_2 = 1e - 05, T = 12$  hours and

$$\begin{aligned} g_1(t) &= -d_1 e^{-\lambda_1 t} + (k_{10} + k_{12}) d_1 e^{-t} - k_{21} d_2 t^\alpha E_{1,1+\alpha}(-t), \\ g_2(t) &= d_2 e^{-t} - k_{12} d_1 e^{-t} + k_{21} d_2 t^\alpha E_{1,1+\alpha}(-t). \end{aligned}$$

The exact solutions are  $\rho_1(t) = d_1 e^{-t}$  and  $\rho_2(t) = d_2 - d_2 e^{-t}$ . Tables 1 and 2 present the errors and convergence rates of errors obtained by the LDG method for  $\alpha = 0.3$  and  $0.7$ , respectively. When  $p = 1, 2$  and  $3$ , the results show that, the convergence rate of the method is  $p + 1$ .

Note that in the following results, are reported where the analytic solutions are not provided. we take  $\tau_i = \frac{1}{2}, i = 1, \dots, n$  and the degree of approximation polynomials is  $p = 3$ . We also apply the Talbot method (see APPENDIX A for a brief review), which is based on the numerical inverse Laplace transform method and compare the results by considering the parameters set as [18].

Table 1: Errors and convergence rate of the LDG method for Example 1 when  $\alpha = 0.35$ .

$\tau$	$\rho_1$		$\rho_2$		CPU time(s)
	$\ e_h\ _{L_2}$	Rate	$\ e_h\ _{L_2}$	Rate	
$p = 2$					
$\frac{1}{2}$	7.832e-01	–	5.820e-01	–	0.48
$\frac{1}{4}$	2.008e-01	1.963	1.466e-01	1.989	0.72
$\frac{1}{8}$	5.082e-02	1.982	3.680e-02	1.994	1.14
$\frac{1}{16}$	1.278e-02	1.991	9.227e-03	1.996	3.31
$\frac{1}{32}$	3.205e-03	1.996	2.312e-03	1.997	14.05
$p = 2$					
$\frac{1}{2}$	1.579e-02	–	2.957e-04	–	0.88
$\frac{1}{4}$	2.019e-03	2.968	1.937e-05	3.932	1.33
$\frac{1}{8}$	2.549e-04	2.985	1.485e-06	3.706	2.09
$\frac{1}{16}$	3.202e-05	2.993	1.396e-07	3.411	8.14
$\frac{1}{32}$	4.012e-06	2.997	1.292e-08	3.433	34.67
$p = 3$					
$\frac{1}{2}$	2.183e-04	–	6.753e-05	–	1.46
$\frac{1}{4}$	1.393e-05	3.970	4.284e-06	3.979	1.82
$\frac{1}{8}$	8.793e-07	3.985	2.823e-07	3.924	4.21
$\frac{1}{16}$	5.539e-08	3.989	2.326e-08	3.601	16.98
$\frac{1}{32}$	3.615e-09	3.938	3.803e-09	2.613	73.33

**Example 2.** Here, we apply the LDG scheme for Eq. (2), when  $u_1(t) = Re^{-\rho t}$ ,  $k_{10} = 0.2$ ,  $k_{12} = 0.6$ ,  $k_{21} = 1$ ,  $R = 2$ ,  $\rho = 2$  and  $T = 48$  hours. Note that, for this case the zero initial condition is considered. The numerical results of the amount of drug in the human body, obtained by the proposed scheme along with results of NILT method (with  $M=80$ ) for different values of  $\alpha$  are illustrated in Figures 1 and 2.

**Example 3.** Consider Eq. (2), in which the parameter set as  $k_{10} = 1$ ,  $k_{12} = 2$ ,  $k_{21} = 0.5$ ,  $u(t) = 0$ ,  $\rho_1 = 100$  mg,  $\rho_2 = 0$  and  $T = 24$  hours. One can see a good match between the results of the proposed scheme and NILT method (with  $M=40$ ) in Figures 3 and 4.

## 5 Conclusion

In the current paper, we have utilized the local discontinuous Galerkin method as a high-order scheme for fractional ODEs which are applicable in pharmacokinetics. This scheme can be easily implemented in a



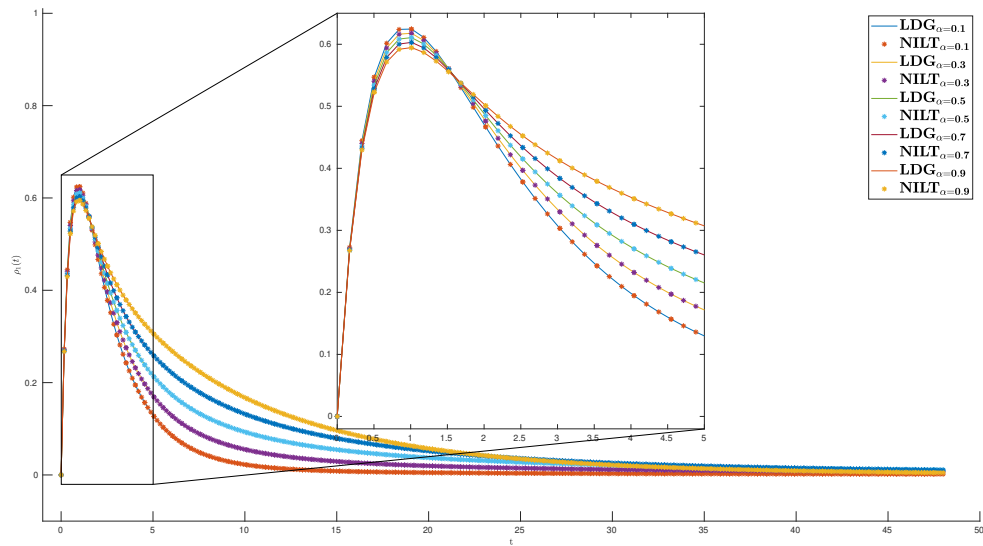


Figure 1: The numerical solutions of the compartment  $\rho_1$  by Eq. (2) with various values of  $\alpha$ .

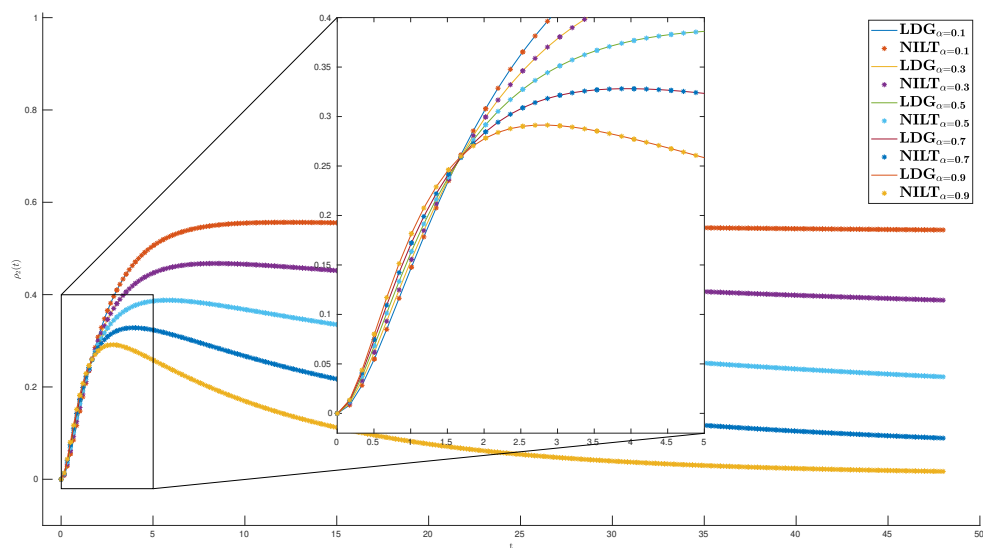


Figure 2: The numerical approximations of the compartment  $\rho_2$  by Eq. (2) with different values of  $\alpha$ .

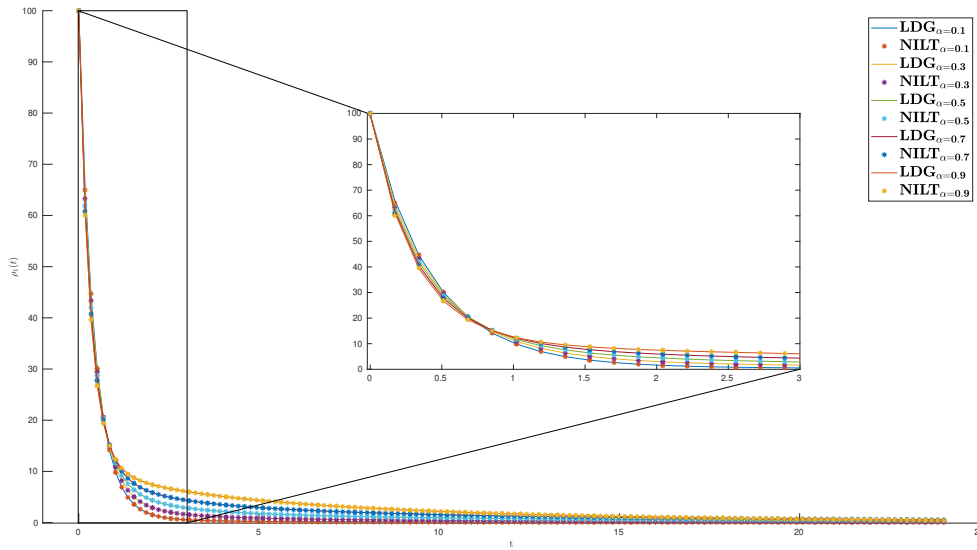


Figure 3: The numerical solutions of the compartment  $\rho_1$  by Eq. (2) with different values of  $\alpha$ .

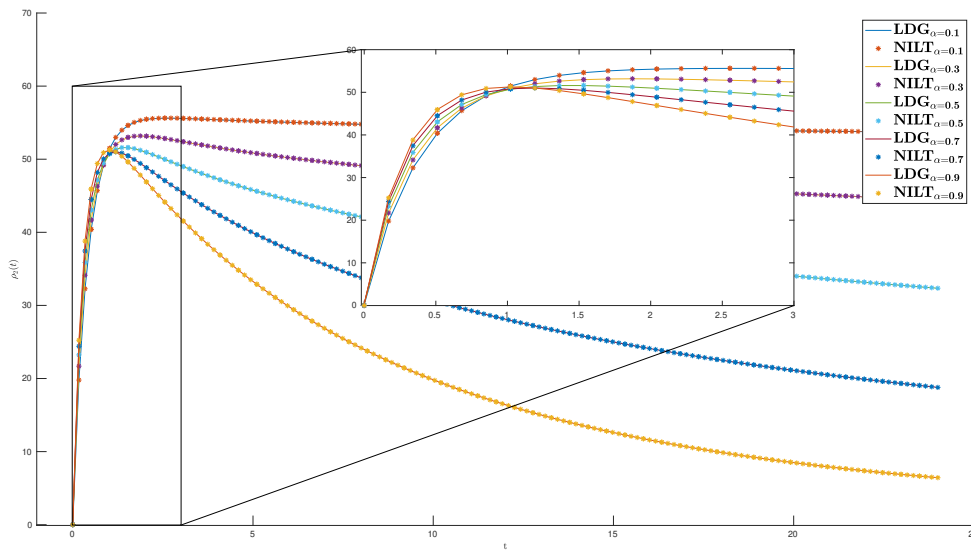


Figure 4: The numerical approximations of the compartment  $\rho_2$  by Eq. (2) with different values of  $\alpha$ .

Table 2: Errors and convergence rate of the LDG method for Example 1 when  $\alpha = 0.70$ .

$\tau$	$\rho_1$		$\rho_2$		CPU time(s)
	$\ e_h\ _{L_2}$	Rate	$\ e_h\ _{L_2}$	Rate	
$p = 1$					
$\frac{1}{2}$	7.771e-01	–	3.408e-01	–	0.45
$\frac{1}{4}$	2.003e-01	1.956	8.572e-02	1.991	0.73
$\frac{1}{8}$	5.081e-02	1.979	2.150e-02	1.995	1.09
$\frac{1}{16}$	1.279e-02	1.990	5.384e-03	1.998	3.17
$\frac{1}{32}$	3.210e-03	1.995	1.347e-03	1.999	13.93
$p = 2$					
$\frac{1}{2}$	1.575e-02	–	4.096e-04	–	0.92
$\frac{1}{4}$	2.018e-03	2.964	2.708e-05	3.919	1.36
$\frac{1}{8}$	2.550e-04	2.985	1.744e-06	3.957	2.2
$\frac{1}{16}$	3.203e-05	2.993	1.109e-07	3.975	8.77
$\frac{1}{32}$	4.013e-06	2.997	7.037e-09	3.979	39.46
$p = 3$					
$\frac{1}{2}$	2.175e-04	–	3.982e-05	–	1.36
$\frac{1}{4}$	1.391e-05	3.967	2.494e-06	3.997	1.83
$\frac{1}{8}$	8.788e-07	3.985	1.564e-07	3.995	4.14
$\frac{1}{16}$	5.520e-08	3.993	9.907e-09	3.981	17.1
$\frac{1}{32}$	3.461e-09	3.996	6.558e-10	3.917	78.97

nodal form (using Lagrange polynomials) or modal form (using Legendre polynomials). We applied the nodal LDG scheme and compare the obtained results with a semi-analytical method based on numerical inverse Laplace transform method. In the LDG method, the order of convergence  $p + 1$ , can be achieved if the  $p$ -th degree of polynomials are used. Here, we get this in practice.

## A Semi-analytic method

In this part, we present a time discretization method based on Laplace transform for Eqs. (2). At first, we recall the following results.

**Theorem 1.** [17] Assuming  $\alpha > 0$ , the LT formula for the Caputo derivative is as follows:

$$\mathcal{L}\{ {}_0^C D_t^\alpha u(t) \} = s^\alpha \tilde{u}(s) - \sum_{k=0}^{n-1} s^{\alpha-k-1} u^{(k)}(0_+), \quad n-1 < \alpha < n, \quad (18)$$

where  $\tilde{u}(s) = \mathcal{L}\{u(t)\}$ .

**Corollary 1.** [17] When  $n = 1$ ,  $0 < \alpha < 1$ , then Eq. (18) reduces to

$$\mathcal{L}\{ {}_0^C D_t^\alpha u(t) \} = s^\alpha \tilde{u}(s) - s^{\alpha-1} u(0_+), \quad 0 < \alpha < 1. \quad (19)$$

Taking Laplace transform from the system of Eqs. (2), gives

$$\begin{aligned} s\tilde{\rho}_1 - \rho_1(0) &= -(k_{10} + k_{12})\tilde{\rho}_1 + k_{21}(s^{1-\alpha}\tilde{\rho}_2 - s^{-\alpha}\rho_2(0)) + \tilde{u}_1, \\ s\tilde{\rho}_2 - \rho_2(0) &= k_{12}\tilde{\rho}_1 - k_{21}(s^{1-\alpha}\tilde{\rho}_2 - s^{-\alpha}\rho_2(0)). \end{aligned} \quad (20)$$

After some manipulation we get

$$\begin{aligned} (s + (k_{10} + k_{12}))\tilde{\rho}_1 - k_{21}s^{1-\alpha}\tilde{\rho}_2 &= \rho_1(0) - k_{21}s^{-\alpha}\rho_2(0) + \tilde{u}_1, \\ -k_{12}\tilde{\rho}_1 + (s + k_{21}s^{1-\alpha})\tilde{\rho}_2 &= (1 + k_{21}s^{-\alpha})\rho_2(0). \end{aligned} \quad (21)$$

The matrix representation of the above system is obtained as

$$\begin{bmatrix} s + (k_{10} + k_{12}) & -k_{21}s^{1-\alpha} \\ -k_{12} & s + k_{21}s^{1-\alpha} \end{bmatrix} \begin{bmatrix} \tilde{\rho}_1(s) \\ \tilde{\rho}_2(s) \end{bmatrix} = \begin{bmatrix} 1 & -k_{21}s^{-\alpha} \\ 0 & 1 + k_{21}s^{-\alpha} \end{bmatrix} \begin{bmatrix} \rho_1(0) \\ \rho_2(0) \end{bmatrix} + \begin{bmatrix} \tilde{u}_1(s) \\ 0 \end{bmatrix}. \quad (22)$$

By using the inverse Laplace transform, the solutions can be shown as:

$$\rho_j(t) = \frac{1}{2\pi i} \int_B e^{st} \tilde{\rho}_j(s) ds, \quad (23)$$

in which  $j = 1, 2$ ,  $i$  is the imaginary unit and  $B$  is the line  $Re(s) = \sigma > \sigma_0$ , known as the Bromwich line [21]. Now, the question arises of how to calculate the integral (23). To address this issue of Talbot's method, for numerically integration of the integral (23) is presented as follows.

### A.1 Talbot's method

The main idea in this method is deformation of the Bromwich line into a curve  $\Gamma$ , such that  $Re(s) \rightarrow -\infty$  on the contour and  $Im(s) \rightarrow \pm\infty$ , in such way the exponential term in the inversion Laplace transform decays rapidly. If so, we consider the following contour

$$\Gamma := \{s : s = \varphi(\theta) + i\sigma\theta, \quad -\infty < \theta < \infty\}, \quad (24)$$

in which  $\sigma$  is a positive real number and  $\varphi$  is a smooth function and is chosen as below [11]

$$\varphi(\theta) = v - \sqrt{\theta^2 + (v - \iota)^2}, \quad \theta \in \mathbb{R}, \quad 0 \leq \iota < v, \quad \sigma > 0. \quad (25)$$

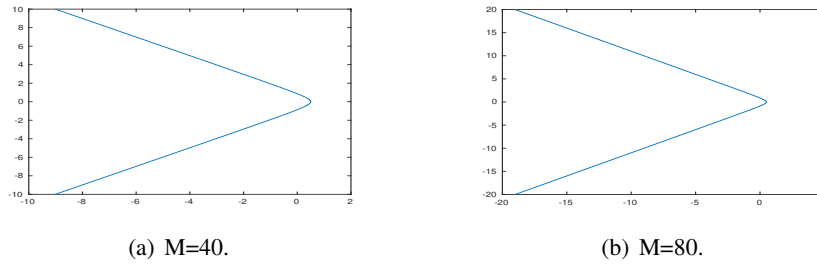


Figure 5: Integration contours  $\Gamma$  when  $\nu = 1$ ,  $\iota = 0.5$ , and  $\sigma = 1$ .

We set  $\theta = (\nu - \iota) \sinh \xi$  and follow the same argument presented in [10, 11], then

$$s(\xi) = \nu - \lambda \sin(\beta - i\xi),$$

in which  $\lambda = (\nu - \iota) \sqrt{1 + \sigma^2}$  and  $\beta = \operatorname{arccot} \sigma$ . Also,  $s'(\xi) = i\lambda \cos(\alpha - i\xi)$ . If so, the Bromwich integral is converted to the following integral with unbounded domain

$$\rho_j(t) = \frac{1}{2\pi i} \int_B e^{st} \tilde{\rho}_j(s) ds = \frac{1}{2\pi i} \int_{-\infty}^{\infty} e^{s(\xi)t} \tilde{\rho}_j(s(\xi)) s'(\xi) d\xi. \tag{26}$$

Now, a quadrature rule like the trapezoidal rule with  $2M + 1$  points is applied and the following result is achieved

$$\begin{aligned} \rho_j^M(t) &\approx \frac{\eta}{2\pi i} \left[ \sum_{m=-M}^M e^{s(\xi_m)t} \tilde{\rho}_j(s(\xi_m)) s'(\xi_m) \right], \\ \eta &= \frac{\log M}{M}, \quad \xi_m = m\eta, \quad -M \leq m \leq M. \end{aligned} \tag{27}$$

**Remark 1.** López-Fernández and Palencia [10] and McLean et al. [11] show that, for  $t > 0$ , the error bound of this integration is of order  $O(e^{-c \frac{M}{\log M}})$ .

The integration contours (24), are shown in Figure 5, when the parameters are chosen as  $\nu = 1$ ,  $\iota = 0.5$ , and  $\sigma = 1$ , for solving Eq. (2).

## References

- [1] B. Cockburn, *Devising discontinuous Galerkin methods for non-linear hyperbolic conservation laws*, J. Comput. Appl. Math. **128** (2001) 187–204.
- [2] B. Cockburn, G. Karniadakis, C.W. Shu, *The development of discontinuous Galerkin methods*, In: Cockburn B, Karniadakis G, Shu CW, editors. *Discontinuous Galerkin Methods: Theory, Computation and Applications. Lecture Notes in Computational Science and Engineering*, 11. New York: Springer-Verlag, 2000, 3–50.
- [3] B. Cockburn, C.W. Shu, *The local discontinuous Galerkin method for time-dependent convection-diffusion systems*, SIAM J. Numer. Anal. **35** (1998) 2440–2463.

- [4] W. Deng, J.S. Hesthaven, *Local discontinuous Galerkin methods for fractional ordinary differential equations*, BIT Numer. Math. **55** (2015) 967–985.
- [5] A. Dokoumetzidis, P. Macheras, *Fractional kinetics in drug absorption and disposition processes*, J. Pharmacokinet. Pharmacodyn. **36** (2009) 165–178.
- [6] A. Dokoumetzidis, R. Magin, P. Macheras, *Fractional kinetics in multi-compartmental systems*, J. Pharmacokinet. Pharmacodyn. **37** (2010) 507–524.
- [7] A. Einstein, *Investigations on the Theory of the Brownian Movement*, Courier Corporation, 1956.
- [8] A.D. Fernández, P. Charchar, A.G. Cherstvy, R. Metzler, M.W. Finnis, *The diffusion of doxorubicin drug molecules in silica nanoslits is non-Gaussian, intermittent and anticorrelated*, Phys. Chem. Chem. Phys. **22** (2020) 27955-27965.
- [9] M. Izadi and M. Afshar, *Solving the Basset equation via Chebyshev collocation and LDG methods*, J. Math. Model. **9** (2021) 61–79.
- [10] M. López-Fernández M and C. Palencia, *On the numerical inversion of the Laplace transform of certain holomorphic mappings*, Appl. Numer. Math. **51** (2004) 289–303.
- [11] W. McLean, I. H. Sloan and V. Thomée, *Time discretization via Laplace transformation of an integro-differential equation of parabolic type*, Numer. Math. **102** (2006) 497–522.
- [12] V. McLean, V. Thomée, *Time discretization of an evolution equation via Laplace transforms*, IMA J. Numer. Anal. **24** (2004) 439–463.
- [13] L. Michaelis and M. L. Menten, *Die kinetik der invertinwirkung*, Biochem. Z. **49** (1913) 333-369.
- [14] H. Mohammadi-Firouzjaei, H. Adibi, M. Dehghan, *Local discontinuous Galerkin method for distributed-order time-fractional diffusion-wave equation: Application of Laplace transform*, Math. Methods Appl. Sci. **44** (2021) 4923-4937.
- [15] K. Mustapha, W. McLean, *Uniform convergence for a discontinuous Galerkin, time-stepping method applied to a fractional diffusion equation*, IMA J. Numer. Anal. **32** (2012) 439–463.
- [16] M.M. Papathanasiou, M. Onel, I. Nascu, E.N. Pistikopoulos, Chapter 6, *Computational tools in the assistance of personalized healthcare*, Vol. 42, Computer Aided Chemical Engineering, 2018, 139–206.
- [17] I. Podlubny, *Fractional Differential Equations: An Introduction to Fractional Derivatives, Fractional Differential Equations, to Methods of Their Solution and Some of Their Applications*, Vol. 198, Elsevier 1998.
- [18] Y. Qiao, H. Xu and H. Qi, *Numerical simulation of a two-compartmental fractional model in pharmacokinetics and parameters estimation*, Math. Methods Appl. Sci. **44** (2021) 11526–11536.
- [19] S.A. Saghir and R.A. Ansari, *Pharmacokinetics*, In: *Reference module in biomedical sciences*, Elsevier, 2018.

- [20] L. Shargel, A.B.C. Yu, *Introduction to Biopharmaceutics and Pharmacokinetics*, McGraw-Hill Education, Seventh Edition, 2012.
- [21] J.A.C. Weideman, L.N. Trefethen, *Parabolic and hyperbolic contours for computing the Bromwich integral*, *Math. Comput.* **76** (2007) 1341–1356.
- [22] P. Sopasakis, H. Sarimveis, P. Macheras and A. Dokoumetzidis, *Fractional calculus in pharmacokinetics*, *J. Pharmacokinet. Pharmacodyn.* **45** (2018) 1341–1356.
- [23] A.V. Weigel, B. Simon, M.M. Tamkun, D. Krapf, *Ergodic and nonergodic processes coexist in the plasma membrane as observed by single-molecule tracking*, *PNAS* **108** (2011) 6438–6443.